Shock Waves (2018) 28:217–225
https://doi.org/10.1007/s00193-017-0761-5

ORIGINAL ARTICLE

A comparison of methods for detonation pressure measurement

J. Pachman[1] · **M. Künzel**[1,2] · **O. Němec**[2] · **J. Majzlík**[1]

Received: 16 February 2017 / Revised: 29 August 2017 / Accepted: 1 September 2017 / Published online: 14 September 2017

Abstract Detonation pressure is an important parameter describing the process of detonation. The paper compares three methods for determination of detonation pressure on the same explosive charge design. Pressed RDX/wax pellets with a density of 1.66 g cm^{-3} were used as test samples. The following methods were used: flyer plate method, impedance window method, and detonation electric effect. Photonic Doppler velocimetry was used for particle velocity measurements in the first two cases. The outputs of the three methods are compared to the literature values and to thermochemical calculation predictions.

Keywords Detonation pressure · Detonation electric effect · Photonic Doppler velocimetry · Impedance matching

1 Introduction

The Zel'dovich–Neumann–Döring detonation model assumes two crucial states in the detonation wave, i.e., the von Neumann (VN) spike, which corresponds to the shock-wave which initiates chemical reactions in the explosive, and the Chapman–Jouguet (CJ) state, which occurs at the end of the reaction zone. The pressure at the CJ state (simply called detonation pressure, p_{CJ}) is one of the most important parameters describing the process of detonation. Experimental determination of this parameter is, however, not widespread, and many new substances are reported with calculated rather than measured values.

The detonation pressure of condensed explosives is in the GPa range, and its direct measurement is therefore difficult to perform. Materials that would directly withstand such a harsh environment long enough to equilibrate without being influenced by strain and temperature effects are not available. The detonation pressure therefore needs to be determined from other experimentally accessible parameters ideally without interfering with the detonation wave.

Two main groups of techniques have emerged over the past few decades that are both based on observation of shock wave properties in well-characterized inert material in contact with an explosive charge. The shock wave generated in the inert material by detonation of an explosive charge can be described by the Hugoniot relation between shock velocity (U) and particle velocity (u) according to the equation

$$U = c_0 + su \tag{1}$$

where c_0 and s are constants describing the inert material under shock loading. The detonation pressure can then be obtained from the knowledge of either shock or particle velocity by applying impedance matching [1] across the explosive–inert interface.

The first of the two groups of techniques mentioned above therefore includes those measuring particle velocities of the inert material adjacent to the explosive charge. The simplest way of particle velocity measurement is a measurement of free-surface velocities of metallic flyers in air or in a vacuum. For the pressure range of interest, the particle velocity can be approximated as half of the free-surface velocity. This approximation has been a subject to thorough exper-

Communicated by A. Higgins.

✉ M. Künzel
kunzel.martin@gmail.com

[1] Institute of Energetic Materials, Faculty of Chemical Technology, University of Pardubice, Studentska 95, 53210 Pardubice, Czechia

[2] OZM Research, s.r.o., Bliznovice 32, 53862 Hrochuv Tynec, Czechia

imental validation [2], and the errors found were around 1% [3,4], provided that the entropy increase associated with the shocked state is small and the material properties in both shocked and unshocked states are the same [5]. Originally, free-surface velocities of metallic flyers were measured using an array of electric pins [6,7] or streak camera recording of argon-filled gaps [8]. A streak camera can also be employed using a wire smear technique [9].

Laser interferometric techniques including Fabry–Perot [10], VISAR [11], and PDV [12] have been used for measurement of particle velocity at the interface between the explosive charge and a transparent inert "window" layer made of either water [13,14], polymethylmethacrylate (PMMA) [15], or lithium fluoride [11,16,17]. The interface is coated with vapour-deposited aluminium [11,17] or simply a thin aluminium foil [13–16] which reflects the laser beam.

The second group of techniques is based on determination of the shock wave velocity. This was done by streak cameras looking at shock waves in water (aquarium test) [18], a moving copper grid in PMMA [19], registering voltage pulses caused by the detonation electric effect [20,21] or more recently by fibre optic probes [22–24]. In all of these experiments, the times at which the shock wave reaches particular positions in the inert material are measured, and dependency of the position versus time is then extrapolated to obtain the shock velocity at zero thickness. The existence of the VN spike is neglected in the evaluation procedure, which might influence the results. The shock wave velocity can also be studied by recording radiation intensity in an inert liquid (CCl_4) for which the dependence of the radiation intensity on the shock pressure is known. This technique is called the photoelectric method [25].

Additionally, techniques based on determination of the particle velocity in the explosive charge itself were also reported using either the electromagnetic induction method [26] or X-rays [27]. The method using electromagnetic particle velocity gauge is based on embedding a thin aluminium bridge in the explosive charge and placing the whole charge in a strong magnetic field. Upon detonation, the current generated in the bridge is proportional to the particle velocity in situ. The X-ray method is based on determination of a metal foil position as it is accelerated by the detonation wave.

Finally, techniques based on embedding a gauge in an inert material also exist, deriving the detonation pressure directly. However, the necessary protection layer of inert material such as polytetrafluorethylene (PTFE) negatively influences the time constant of the measurements. Manganin gauges [28] as well as carbon resistor gauges [29] are used.

The goal of this article is to compare three methods that can be relatively easily used to experimentally characterize new explosives. The flyer plate method (FPM) and impedance window method (IWM) were instrumented with a photonic Doppler velocimeter [30]. The third method is based on the detonation electric effect (DEM). It allows registering shock wave position in a layered PMMA block placed on the charge. Evaluation of raw experimental data is discussed, and possible sources of measurement uncertainty are pointed out. The acquired results are compared to those found in the existing literature and also to calculations using a thermochemical code.

2 Experimental details

The explosive charges were made of pressed RDX-based explosive designated A-IX-1 (95% RDX + 3% ceresine + 2% stearine + trace amount of orange dye). The charges were pressed to a density (ρ_0) of $1.66 \pm 0.01\,\mathrm{g\,cm^{-3}}$, i.e., 96% of their theoretical maximum density. The detonation velocity (D) was determined separately by fibre optic probes [22,31]. The average value of four shots was $8238 \pm 19\,\mathrm{m\,s^{-1}}$. The booster charge was made of 40 g of Semtex 1A plastic-bonded explosive based on pentaerythritol tetranitrate. The length-to-diameter ratio (l/d) of the charges including booster was 1.5 in the case of FPM and IWM and 2 in the case of DEM. Some shots were also performed with FPM at $l/d = 1.2$ and $l/d = 4$. The charge diameter was 40 mm (FPM, IWM) or 50 mm (DEM).

2.1 Set-up of the experiments

The flyer plate (Fig. 1a) and impedance window (Fig. 1b) experiments followed similar experimental set-ups. The explosive charge was placed in the vertical position with booster and detonator fixed to its bottom. The aluminium flyer was placed on the upper surface of the charge. The PDV probe was supported by a holder made of polystyrene foam. The thicknesses of the flyers varied from 0.03 to 15 mm (all shown in Fig. 3). The flyers were made of aluminium alloy EN AW-1050, which consist of 99.5% aluminium and trace amounts of other elements, mostly iron and silicon. The flyers were mostly prepared by water jet cutting using plates or foils except the first series of shots (charges with $l/d = 1.5$, flyer thickness over 4 mm) where they were machined from round stock. In some experiments, the flyers were glued to the charges using epoxy resin, which led to improved signal quality.

In case of IWM experiments (Fig. 1b), a mirror layer of aluminium self-adhesive foil followed by a PMMA window was placed on the upper surface of the charge. The thickness of the aluminium foil was 30 μm with a 20 μm layer of acrylic glue, and the window thickness was 3.3 or 10 mm. The sticky side of the foil was oriented towards the window. The space between the foil and the charge was filled with ~10-μm-thick layer of silicone grease or epoxy.

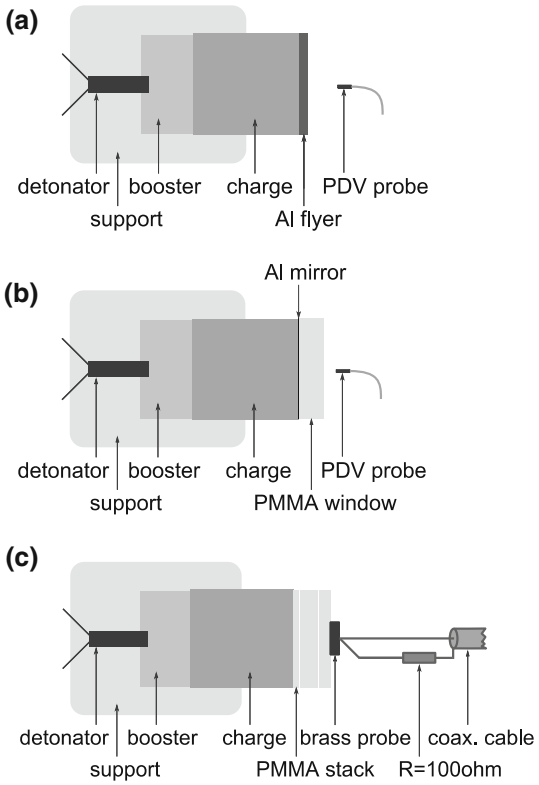

Fig. 1 Scheme of the FPM (**a**), IWM (**b**), and DEM (**c**) experimental arrangements

For detonation electric effect measurements (DEM), the stack of 9 PMMA plates with dimensions of $50 \times 50 \times 3$ mm was placed on the top surface of the charge (Fig. 1c). Thin air layers with thickness of 20–30 μm between the PMMA plates were fixed with glue. The brass capacitive probe was placed on the stack and connected to the oscilloscope using a short length of coaxial cable (4 m). The probe was grounded via 100 Ω resistor.

2.2 Photonic Doppler velocimetry

The photonic Doppler velocimetry [32] measurements of free-surface velocities and interface velocities were taken using a single-channel PDV system [30], which is now being commercialized by OZM research. It was a first-generation system with a reference signal taken from the probe back reflection. The detector signal was recorded using a high-bandwidth Tektronix oscilloscope (DPO70000 series). The laser was operated at nominally 1550 nm with an optical power output of 36 mW. The laser light was pointed to the target by means of collimating probes, flat-end fibre connectors or preferably bare cleaved fibre probes. The probes were fixed in a position perpendicular to the flyer or impedance window surface and approximately 5 mm above it. The oscilloscope records were analysed using short-time Fourier transform (STFT) with a Hamming window. The window parameters were set in a way that the time and velocity resolution based on the STFT uncertainty principle [33] were 5 or 10 ns and 30 or 15 m s^{-1}, respectively.

2.3 Calculation of detonation parameters

Calculation of detonation parameters was conducted using the latest available version of the Explo5 V6.03 thermochemical code [34]. The code uses fundamental fluid Exp-6 equation of state (EOS) according to Byers–Brown's approach for the description of detonation products [35].

3 Results

3.1 Metal acceleration experiments

A series of metal plate acceleration experiments with aluminium plates of various thicknesses were conducted. Using velocity profiles obtained from these experiments, attenuation of the initial shock in aluminium is revealed which allows gaining information on the particle velocity profile in the detonation wave of the explosive. The evaluation of plate acceleration results was principally performed in the same way as in the original article by Duff and Houston [6] by plotting first jump-off (free-surface) velocities of all plates against plate thickness b (Fig. 3).

The first part of the graph has a steep slope because of the influence of the original shock in the explosive which corresponds to the VN spike. The latter part of the graph corresponds to the expansion of reaction products behind the CJ state (Taylor wave). Both parts were fitted with regression lines (A and C in Fig. 3), and the intersection of the lines marked the flyer plate thickness corresponding to that at which the VN spike just attenuated (b_{CJ}). The data points were also fitted with a second-order exponential decay function

$$y = 1.642\ \mathrm{e}^{-x/0.409} + 1.616\ \mathrm{e}^{-x/18.832} + 1.358 \qquad (2)$$

which provided good fit quality with the coefficient of determination $R^2 = 0.990$. All coefficients of linear regression lines are listed in Table 1.

Table 1 Coefficients of linear regression lines ($y = ax + b$) used in Fig. 3

Line	l/d	a	b	R^2
A	1.5	−2047.1	4419.5	0.921
B	4	−48.235	3172.4	1
C	1.5	−63.523	2960.7	0.938
D	1.2	−67.250	2807.0	0.989

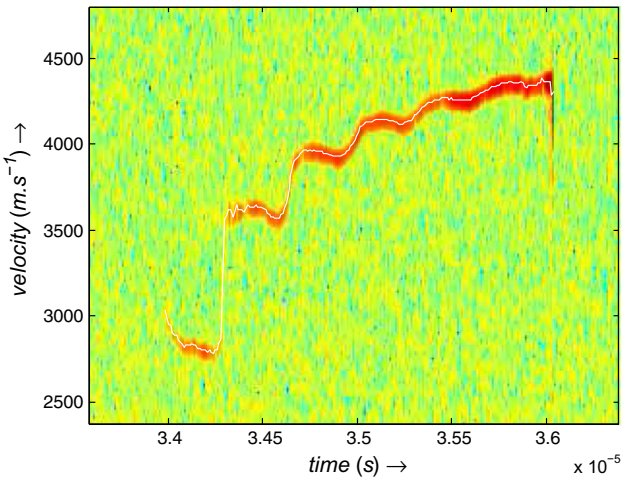

Fig. 2 Example of PDV velocity spectrogram obtained by Fourier transform with a time resolution of 10 ns. The flyer thickness was 1 mm. The step-like acceleration of the plate caused by shock reverberations is clearly visible

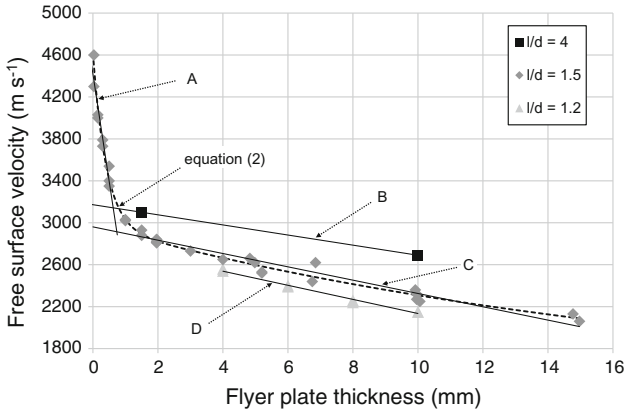

Fig. 3 Aluminium flyer free-surface velocities for various plate thicknesses

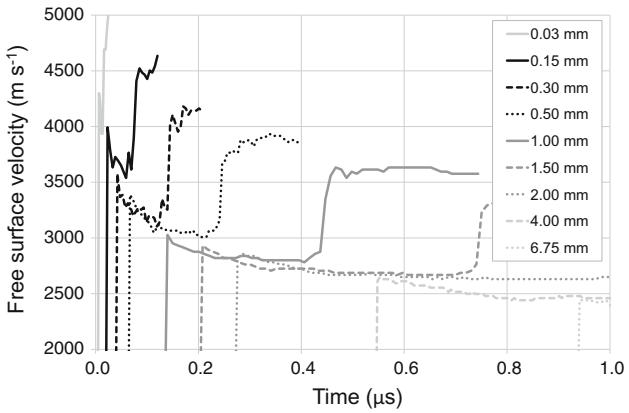

Fig. 4 Free-surface velocity profiles of aluminium flyers shifted in time by taking into consideration shock wave attenuation in aluminium. The latter records were shifted using shock wave velocities determined from the former records. The flyers thicker than 7 mm were omitted for clarity

The free-surface velocities were assumed to be twice the particle velocities in the material. Extrapolation of the exponential fit to zero plate thickness provided an estimate of the peak value of $u_{\text{VN-Al}} = 2308 \pm 75$ m s^{-1}. The particle velocity corresponding to the CJ state transferred to aluminium $u_{\text{CJ-Al}} = 1595 \pm 18$ m s^{-1} was read from the exponential fit at $b = b_{\text{CJ}}$. However, this value might have been negatively influenced by large shock wave curvature and subsequent energy losses which are present at low length-to-diameter ratio of the charge ($l/d = 1.5$). It was shown by [36] that the Taylor wave pressure is inversely proportional to the detonation wave curvature, which is influenced by l/d ratio and charge confinement. Significant decrease in detonation wave curvature of A-IX-1 explosive was confirmed when l/d was increased from 1.5 to 4 [37]. Therefore, two additional FPM experiments were performed with long charges ($l/d = 4$), which resulted in the particle velocity value of $u_{\text{CJ-Al}} = 1641 \pm 18$ m s^{-1}. Some shots were also performed at $l/d = 1.2$ with all the resulting velocities being lower than the corresponding values at $l/d = 1.5$ (Fig. 3). The example spectrogram is shown in Fig. 2.

The PDV instrumentation enabled us to capture the actual velocity profiles of all experiments. The representative free-surface velocity profiles that were shifted in time by taking into consideration shock wave attenuation in aluminium are shown in Fig. 4. The measured particle velocities were used to calculate shock velocities in aluminium plates of corresponding thicknesses using the Hugoniot equation (1) with constants $\rho_{\text{Al}} = 2.70 \pm 0.01$ g cm^{-3}, $c_{0\text{-Al}} = 5.35$ km s^{-1}, and $s_{\text{Al}} = 1.32$ taken from [38]. The dependence of shock velocity on the aluminium flyer thickness was determined and approximated by an exponential regression curve. The time shifts were then determined based on plate thickness and corresponding mean shock velocity using equation

$$t_b = b^{-2} \int_0^b U_{\text{Al}}(x)\,\mathrm{d}x \tag{3}$$

where t_b is the time shift for the plate with thickness b, and U_{Al} is the actual shock velocity obtained from the free-surface velocity-flyer plate thickness profiles. Figure 4 is to be compared with results of [12] where a similar sequence of particle velocity profiles was obtained by numerical simulations.

The available data on particle velocities of various flyers allowed us to estimate reaction zone thickness (a) and duration (t_{RZ}) of the explosive. The evaluation was performed in the same manner as by Duff and Houston [6] using the equation

$$a = b_{\text{CJ}} \frac{[D\,(u_{\text{CJ-Al}} + U_{\text{CJ-Al}} - U_{\text{m-Al}})\,(1 - u_{\text{m-Al}}/D)]}{[U_{\text{m-Al}}\,(u_{\text{CJ-Al}} + U_{\text{CJ-Al}} - u_{\text{m-Al}})]} \tag{4}$$

$$t_{\mathrm{RZ}} = a/D \tag{5}$$

where b_{CJ} is the distance (flyer thickness) required for the breakpoint of the unloading wave corresponding to the CJ plane to overtake the shock wave in the flyer, $u_{\text{CJ-Al}}$ and $U_{\text{CJ-Al}}$ are particle and shock velocities corresponding to the CJ plane transferred to the flyer, u_{m} and U_{m} are the mean particle and shock velocities corresponding to the original shock in the flyer. The latter two parameters were determined using equation

$$u_{\text{m-Al}} = b_{\mathrm{CJ}}^{-1} \int_0^{b_{\mathrm{CJ}}} u_{\mathrm{Al}}\,(x)\,\mathrm{d}x \tag{6}$$

where u_{Al} is the actual particle velocity in the flyer. An analogous equation was used for U_{Al}. The resulting values of $t_{\mathrm{RZ}} = 10 \pm 2$ ns and $a = 0.084 \pm 0.016$ mm were obtained for charges with $l/d = 1.5$ using FPM.

3.2 PMMA window experiments

The particle velocity profile obtained from the PDV signal corresponds to the PMMA particle velocity at the interface with the explosive. The example spectrogram is shown in Fig. 5. Eight shots were performed with the same experimental arrangement. The peak particle velocity value transferred to the window of $u_{\text{VN-PMMA}} = 3336 \pm 80$ m s^{-1} is assumed to roughly correspond to the VN spike peak value. The particle velocity corresponding to the CJ state transferred to the window $u_{\text{CJ-PMMA}} = 2525 \pm 61$ m s^{-1} was read from the closest data point above the intersection of the regression lines of the initial VN spike and the following Taylor wave (Fig. 6). No correction coefficient for shock-induced change of refractive index was applied as its value for PMMA is equal to 1 ± 0.01 according to available literature [39,40].

According to [15], reaction zone thickness can be estimated from particle velocity profiles according to the relation

$$a < (D - u_{\text{CJ-PMMA}})\, t_{\mathrm{ap}} \tag{7}$$

where D is the detonation velocity of the explosive, $u_{\text{CJ-PMMA}}$ is the particle velocity corresponding to the CJ plane transferred to the window, and t_{ap} is the apparent duration of the initial VN spike read from the particle velocity profile. We modified this relation to the form of equation

$$a = \left(D - \left(t_{\mathrm{ap}}^{-1} \int_0^{t_{\mathrm{ap}}} u_{\mathrm{PMMA}}\,(x)\,\mathrm{d}x \right) \right) t_{\mathrm{ap}} \tag{8}$$

where u_{PMMA} is the actual particle velocity obtained from the measured particle velocity–time profiles. The values of $t_{\mathrm{RZ}} = 21 \pm 2$ ns and $a = 0.174 \pm 0.018$ mm were found for charges with $l/d = 1.5$ using IWM.

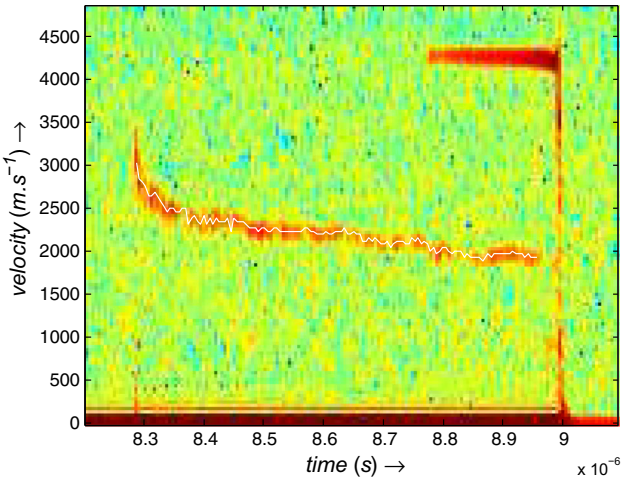

Fig. 5 Example of PDV velocity spectrogram obtained by Fourier transform with time resolution of 5 ns. The velocity trace at about 4250 m s^{-1} corresponds to movement of the window/air interface before it hits the probe

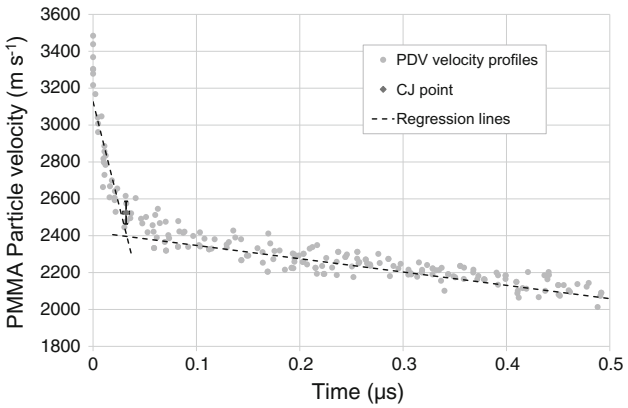

Fig. 6 Particle velocity profiles at the explosive/PMMA interface of eight identical charges. The linear regression lines corresponding to the VN spike and Taylor wave are shown for one of the profiles. The CJ point determined as the closest data point above the intersection of the two regression lines is shown. The median absolute deviations of time and particle velocity are indicated

3.3 PMMA shock velocity experiments

Four charges were tested using DEM, of which two gave reasonable results. The voltage signals captured on the oscilloscope had typical profiles containing the initial voltage step followed by a series of voltage drops (Fig. 7). The number of voltage drops corresponds to the number of air gaps between the PMMA plates. The time intervals of shock passage through successive plates were read out between the onsets of voltage derivative peaks and plotted against the total distance travelled. Quadratic regression was then applied, and the PMMA shock wave velocity at zero plate thickness was found as the first derivative of the curve at time $t = 0$ as is shown in Fig. 8. The mean value of $U_{\text{CJ-PMMA}} =$

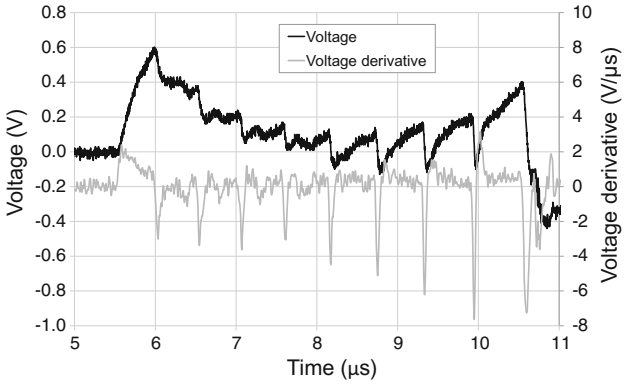

Fig. 7 Typical raw signal obtained by DEM and its first derivative. The shock wave transition times corresponding to the PMMA plates were read out at the onsets of the derivative peaks

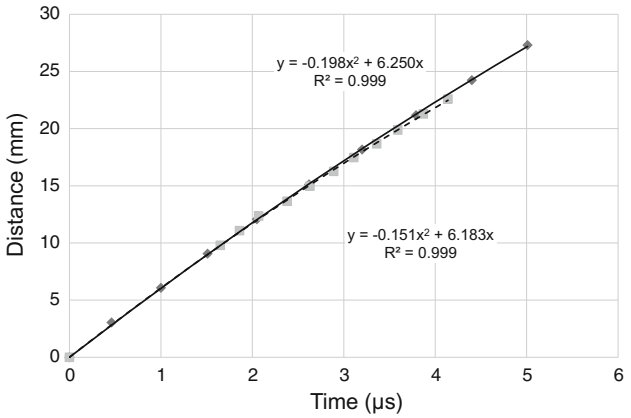

Fig. 8 Shock wave position versus time data for the two DEM experiments. The first derivative at $t = 0$ was considered the PMMA shock velocity (mm μs^{-1}) corresponding to the CJ state

6217 ± 61 ms^{-1} was found. The uncertainties of the shock wave velocity measurement were in this case estimated not only from the small number of shots performed with A-IX-1 but from a dataset obtained with similar RDX-based pressed charges. The PMMA particle velocity was then calculated using the Hugoniot equation (1) where the material constants $\rho_{\text{PMMA}} = 1.186$ g cm^{-3}, $c_{0\text{-PMMA}} = 2.598$ km s^{-1}, and $s_{\text{PMMA}} = 1.516$ were taken from [41]. It was discussed in [21] that the zero point should be omitted from the regression because the first peak has a reversed polarity and much lower intensity compared to the others. Unfortunately, the original raw signal is not shown. We believe that there is no doubt about the first voltage step in our case.

3.4 Determination of CJ detonation pressure

The particle velocity data were used to calculate the detonation pressure by means of the impedance matching technique. Cooper's generalized EOS for detonation products [41]

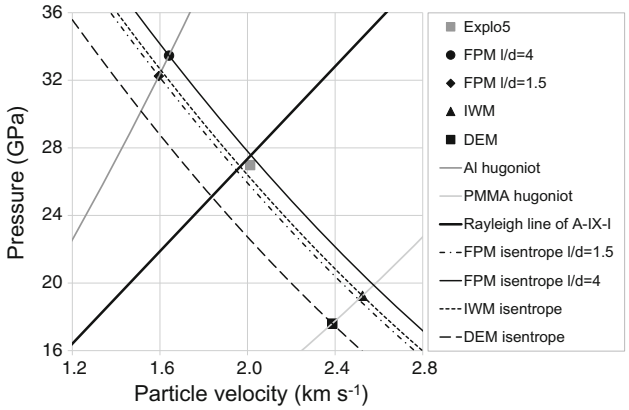

Fig. 9 Detailed view of the impedance matching diagram shows graphical determination of the CJ detonation pressure. Experimental data points obtained using FPM, IWM, and DEM are shown. The particular CJ conditions are found at the intersections of the Rayleigh line and the corresponding isentropes

$$p/p_{\text{CJ}} = 2.412 - 1.7315\,(u/u_{\text{CJ}}) + 0.3195\,(u/u_{\text{CJ}})^2 \qquad (9)$$

was fitted to the measured data according to the graphical procedure which is described in [12]. The trial p_{CJ} and u_{CJ} parameters which fulfil the Rayleigh line equation

$$p_{\text{CJ}} = \rho_0\, D\, u_{\text{CJ}} \qquad (10)$$

were input to (9) until the resulting curve passed through the measured $u_{\text{CJ-PMMA}}$ or $u_{\text{CJ-Al}}$ and the corresponding pressure values substituted for u and p. The Hugoniot curves of Al and PMMA were constructed using the above-mentioned constants taken from [38,41]. The impedance matching diagram is shown in Fig. 9.

4 Discussion

The CJ parameters of the tested explosive obtained by the three methods are presented in Table 2. Medians and median absolute deviations are used for mean values and repeatability limits, respectively, through the whole paper.

From the FPM free-surface velocity profiles, it can be clearly seen that the Taylor wave shifts down with decreasing l/d. The overall repeatability of the free-surface velocity measurements resulted in an uncertainty of the final p_{CJ} of 0.9%, which is comparable to less than 1% repeatability achieved by [12]. Poor repeatability achieved with the thick machined flyers in the first few tests led us to use the flyers made by water jet cutting of plates. Nevertheless, the repeatability achieved with these flyers slightly decreases with decreasing thickness.

Although the velocity resolution of the PDV records is inherently limited by the use of STFT for data evaluation, the

Table 2 Comparison of the data obtained by the three methods, some literature sources, and Explo5 calculation results

Method	ρ (g cm^{-3})	D (m s^{-1})	l/d	u_{CJ} (m s^{-1})	p_{CJ} (GPa)
FPM	1.66 ± 0.01	8238	1.5	1945 ± 18	26.60 ± 0.25
FPM	1.66 ± 0.01	8238	4.0	2011 ± 18	27.50 ± 0.25
IWM	1.66 ± 0.01	8238	1.5	1981 ± 33	26.89 ± 0.46
DEM	1.66 ± 0.01	8238	2.0	1836 ± 40	25.11 ± 0.55
Aquarium [44][a]	1.63	8341	3.0	2087 ± 81	28.4 ± 1.1
Photoelectric [25][a]	1.67	8300	1.0	2085	28.9
Inductive [45]	1.65	8265	2.0	1808	24.6
Inductive [45]	1.68	8425	2.0	1851	26.1
Explo5	1.66	8078	–	2012	26.98
Explo5[a]	1.66	8216	–	2105	28.72

The uncertainties are median absolute deviations of repeated experiments except the case of [44] where standard deviations were provided
[a] Pure RDX

situation is not as bad as the uncertainty principle predicts. It was shown by [42] that the real limiting resolution of the PDV signals is about one-fifth of the uncertainty principle prediction, i.e., in case of FPM the uncertainty introduced by the spectrogram reading should be about 0.1%. The p_{CJ} value obtained at $l/d = 4$ must be considered with care because of the small number of experimental points.

The FPM reveals full particle velocity profile from multiple shots, which is both expensive and time-consuming. If just the CJ parameters are desired, the approach of a proper analysis of single shots using thin plate acceleration as is described in [12] appears to be more reasonable. Figure 4 shows that the flyer plate thickness at which the VN spike of A-IX-1 fully attenuates in aluminium is 1–1.5 mm.

The advantage of using IWM is that it reveals the full particle velocity profile within a single experiment directly at the explosive's interface, which makes it less sensitive to non-ideal charge geometry. The p_{CJ} value found for charges with $l/d = 1.5$ was close to the Explo5 prediction.

The repeatability of the p_{CJ} measurement using IWM was 1.7%. The scatter of the measured particle velocity profiles is probably caused by combined effects of detonation front structure, explosive surface roughness, and some variability of the PDV signal quality. It might also be influenced by shock reverberations in the aluminium layer although the shock round-trip time in it is less than 8 ns. The missing window correction factor possibly introduces some additional systematic error of less than 1%. The spectrogram reading error is in this case estimated to 0.25% of the actual value.

The DEM is the cheapest and simplest option for CJ pressure measurement of the three. The principal disadvantage of the method is that it neglects the VN spike and does not provide the full pressure–time profile of the detonation wave. The resulting CJ pressure is slightly lower compared to the other results, and the repeatability of the DEM results (2.2% of the CJ pressure) is lower compared to the IWM and FPM.

Moreover, although the regression curves fit well to the data points ($R^2 > 0.99$), their derivations are extremely sensitive. For example, if any data point is omitted, the terms change by several per cent. Performing other than parabolic regression also leads to large changes in the resulting p_{CJ} values. The factors that influence the shock attenuation are the triangular shape of the loading pulse, shock interaction with the air gaps between the PMMA plates, and visco-elastic loss in PMMA. Additional effect of lateral release waves may appear at the PMMA thickness $b_{PMMA} > d/2$ [43].

For comparison, calculations were performed using the Explo5 thermochemical code. Some literature data are also shown, which were obtained for pure pressed RDX by the aquarium test [44] and photoelectric method [25] and for A-IX-1 by the inductive method [45]. The CJ pressures we obtained are in good agreement with the corresponding Explo5 code values. The differences to some of the literature values can be attributed to the presence of a binder component in the A-IX-1. In accordance with the calculations, the presence of 5% of waxy binder in the pressed RDX decreases its CJ detonation pressure by about 6%.

The reaction zone length estimations by FPM (0.08 mm) and IWM (0.17 mm) are not consistent. It must be noted that the FPM result is inherently underestimated, and the IWM result is overestimated due to the impedance mismatch between the explosive and the adjacent inert material. The only available literature value for comparison was 0.28 mm [25], but it is believed to be inaccurate due to poor resolution and complexity of the experimental method.

The true peak value of the von Neumann spike cannot be properly determined using either FPM or IWM. The major problem is again the impedance mismatch, which causes the reaction zone in the explosive to interact with the shock (FPM) or release (IWM) wave reflected back from the interface. In the case of FPM, there is also an uncertainty introduced by extrapolation of the data to zero flyer thickness

coupled with the velocity scatter of thin flyer measurements. Another limiting factor for IWM is the PDV spectrogram reading error, which may reach several per cent in the case of the first jump-off velocity.

5 Conclusions

The three methods of detonation pressure measurement were used for pressed RDX charges. The flyer plate (FPM) and the impedance window (IWM) methods were instrumented with PDV diagnostics, which allowed us to obtain high-resolution velocity profiles. The difference in CJ pressures obtained using these two methods for charges with $l/d = 1.5$ was less than 1%, and they were about 1% below the thermochemical code prediction. The FPM allows a good quality particle velocity profile to be obtained from approximately 10 shots. The IWM reveals the full particle velocity profile of the detonation wave from a single experiment. The pressure determined by the method based on the detonation electric effect (DEM) is almost 7% lower compared to the others, and the result largely depends on the type of data regression. The IWM seems to be the most effective method among the three. The uncertainty of its results might be further improved by careful preparation of the tested charges and by proper determination of the window correction factor for PMMA.

Acknowledgements Financial support for this work from the Technology Agency of the Czech Republic Project TA02010923 is gratefully acknowledged.

References

1. McQueen, R.G., Marsh, S.P., Taylor, J.W., Fritz, J.N., Carter, W.J.: The equation of state of solids from shock wave studies. In: Kinslow, R. (ed.) High-Velocity Impact Phenomena, p. 293. Academic Press, New York (1970)
2. Rice, M.H., McQueen, R.G., Walsh, J.M.: Compression of solids by strong shock waves. Solid State Phys. **6**, 1–63 (1958). doi:10.1016/S0081-1947(08)60724-9
3. Walsh, J.M., Christian, R.H.: Equation of state of metals from shock wave measurements. Phys. Rev. **97**, 1544 (1955). doi:10.1103/PhysRev.97.1544
4. Walsh, J.M., Rice, M.H., McQueen, R.G., Yarger, F.L.: Shock-wave compressions of twenty-seven metals. Equations of state of metals. Phys. Rev. **108**, 196 (1957). doi:10.1103/PhysRev.108.196
5. Ahrens, T.J.: MateriaI strength effect in the shock compression of alumina. J. Appl. Phys. **39**, 4610 (1968). doi:10.1063/1.1655810
6. Duff, R.E., Houston, E.: Measurement of the Chapman–Jouguet pressure and reaction zone length in a detonating high explosive. J. Chem. Phys. **23**(7), 1268–1273 (1955). doi:10.1063/1.1742255
7. Goranson, R.W.: A Method for Determining Equations of State and Reaction Zones in Detonation of High Explosives, and Its Application to Pentolite, Composition B, Baratol and TNT. Report LA-487. Los Alamos, USA (1946)
8. Deal, W.E.: Measurement of Chapman–Jouguet pressure for explosives. J. Chem. Phys. **27**(1), 796–800 (1957). doi:10.1063/1.1743831
9. Davis, W.C., Craig, B.G.: Smear camera technique for free-surface velocity measurement. Rev. Sci. Instrum. **32**, 579 (1961). doi:10.1063/1.1717443
10. Fedorov, A.V., Mikhailov, A.L., Antonyuk, L.K., Nazarov, D.V., Finyushin, S.A.: Determination of chemical reaction zone parameters, Neumann peak parameters, and the state in the Chapman–Jouguet plane in homogeneous and heterogeneous high explosives. Combust. Explos. Shock Waves (Engl. Transl.) **48**(3), 302–308 (2012). doi:10.1134/S0010508212030070
11. Bouyer, V., Doucen, M., Decaris, L.: Experimental measurements of the detonation wave profile in a TATB based explosive. EPJ Web Conf. **10**, 00030 (2010). doi:10.1051/epjconf/20101000030
12. Lorenz, K.T., Lee, E.L., Chambers, R.: A simple and rapid evaluation of explosive performance—the disc acceleration experiment. Propellants Explos. Pyrotech. **40**(1), 95–108 (2015). doi:10.1002/prep.201400081
13. Sheffield, S.A., Blomquist, D.D.: Subnanosecond measurements of detonation fronts in solid high explosives. J. Chem. Phys. **80**(8), 3831–3844 (1984). doi:10.1063/1.447164
14. Utkin, A.V., Mochalova, V.M., Logvinenko, A.A.: Effect of diethylenetriamine on the structure of detonation waves in nitromethane. Combust. Explos. Shock Waves (Engl. Transl.) **49**(4), 478–483 (2013). doi:10.1134/S0010508213040114
15. Yunoshev, A.S., Plastinin, A.V., Silvestrov, V.V.: Effect of the density of an emulsion explosive on the reaction zone width. Combust. Explos. Shock Waves (Engl. Transl.) **48**(3), 319–327 (2012). doi:10.1134/S0010508212030094
16. Gustavsen, R.L., Bartram, B.D., Sanchez, N.J.: Detonation wave profiles measured in plastic bonded explosives using 1550 nm photon Doppler velocimetry. AIP Conf. Proc. **1195**, 253 (2010). doi:10.1063/1.3295117
17. Fedorov, A.V.: Detonation wave structure in liquid homogeneous, solid heterogeneous and agatized HE. Paper presented at the Twelfth International Symposium on Detonation, San Diego, California, USA, 11–16 Aug (2002)
18. Cook, M.A., Keyes, R.T., Ursenbach, W.O.: Measurements of detonation pressure. J. Appl. Phys. **33**(12), 3413–3421 (1962). doi:10.1063/1.1702422
19. Held, M.: Determination of the Chapman–Jouguet pressure of a high explosive from one single test. Def. Sci. J. **37**(1), 1–9 (1987). doi:10.14429/dsj.37.5886
20. Hayes, B.: The detonation electric effect. J. Appl. Phys. **38**(2), 507–511 (1967). doi:10.1063/1.1709365
21. Green, L.G., Lee, E.L.: Detonation pressure measurements on PETN. Paper presented at the 13th International Detonation Symposium, Norfolk, Virginia, USA, 23–28 July (2006)
22. Prinse, W.C., Esveld, L., Oostdam, R., Roojien, M., Bouma, R.: Fibre-optical techniques for measuring various properties of shock waves. Paper presented at the 23rd International Congress on High-Speed Photography and Photonics, Moscow, Russia, 20 Sept (1998). doi:10.1117/12.350497
23. Krupka, M.: OPTIMEX—scientific report of the progress and results obtained in 2015. In: Technology Agency of Czech Republic, Hrochuv Tynec (2015) **(in Czech)**
24. Krupka, M., Pachman, J., Selesovsky, J., Marsalek, R., Pospisil, M.: OPTIMEX—fiber optical system for EM performance. Paper presented at the Greener and Safer Energetic and Ballistic Systems (GSEBS), Bucharest, Romania, 22–23 May (2016)
25. Loboiko, B.G., Lubyatinsky, S.N.: Reaction zones of detonating solid explosives. Combust. Explos. Shock Waves (Engl. Transl.) **36**(6), 716–733 (2000). doi:10.1023/A:1002898505288
26. Cowperthwaite, M., Rosenberg, J.T.: Lagrange gage studies in ideal and non-ideal explosives. Paper presented at the Seventh Sympo-

sium (International) on Detonation, Annapolis, Maryland, USA, 16–19 June (1981)
27. Rivard, W.C., Venable, D., Fickett, W., Davis, W.C.: Flash X-ray observation of marked mass points in explosive products. Paper presented at the Fifth International Symposium on Detonation, Pasadena, California, USA (1970)
28. Vantine, H., Chan, J., Erickson, L., Janzen, J., Weingart, R., Lee, R.: Precision stress measurements in severe shockwave environments with low-impedance manganin gauges. Rev. Sci. Instrum. **51**, 116–122 (1980). doi:10.1063/1.1136038
29. Watson, R.W.: Gauge for determining shock pressures. Rev. Sci. Instrum. **38**, 978–980 (1967). doi:10.1063/1.1720946
30. Pachman, J., Künzel, M., Němec, O., Bland, S.: Characterization of Al plate acceleration by low power photonic Doppler velocimetry (PDV). Paper presented at the 40th International Pyrotechnics Society Seminar, Colorado Springs, USA, 13–18 July (2014)
31. Künzel, M., Matyáš, R., Vodochodský, O., Pachman, J.: Explosive properties of melt cast erythritol tetranitrate. Cent. Eur. J. Energy Mater. (2017). doi:10.22211/cejem/68471
32. Strand, T., Goosman, D.R., Martinez, C., Whitworth, T.L., Kuhlow, W.W.: Compact system for high-speed velocimetry using heterodyne techniques. Rev. Sci. Instrum. **77**, 083108 (2006). doi:10.1063/1.2336749
33. Strand, T., Kuhlow, B.: Resolution capabilities of the Fourier transform method for PDV. Paper presented at the Photonic Doppler Velocimetry Workshop, Livermore, California, USA, 20–21 July (2006)
34. Sućeska, M.: Explo5 Version 6.03/2016 User's Guide. OZM Research (2016)
35. Brown, W.B.: Analytical representation of the excess thermodynamic equation of state for classical fluid mixtures of molecules interacting with α-exponential-six pair potentials up to high densities. J. Chem. Phys. **87**(1), 566–577 (1987). doi:10.1063/1.453605
36. Craig, B.G.: Measurement of detonation-front structure in condensed-phase explosives. Paper presented at the Tenth Symposium (International) on Combustion, Cambridge, UK (1965). doi:10.1016/S0082-0784(65)80230-2
37. Pachman, J., Künzel, M., Kubát, K., Selesovsky, J., Maršálek, R., Pospíšil, M., Kubíček, M., Prokeš, A.: OPTIMEX: Measuring of detonation front curvature with passive fiber optical system. Cent. Eur. J. Energy Mater. **13**(4), 808–820 (2016). doi:10.22211/cejem/62776
38. Choudhury, D., Gupta, Y.M.: Shock compression and unloading response of 1050 aluminum to 70 GPa. AIP Conf. Proc. **1426**, 755 (2012). doi:10.1063/1.3686388
39. Chapman, D.J., Eakins, D.E., Williamson, D.M., Proud, W.G.: Index of refraction measurements and window corrections for PMMA under shock compression. AIP Conf. Proc. **1426**, 442 (2012). doi:10.1063/1.3686313
40. Gustavsen, R.L., Bartram, B.D., Sanchez, N.: Shock initiation measurements using multiple samples & instrumented with PDV. Paper presented at the Photonic Doppler Velocimetry Workshop, Austin, Texas, USA, 5–6 Nov (2009)
41. Cooper, P.W.: Explosives Engineering. Wiley-WCH Inc, New York (1996)
42. Dolan, D.H.: Accuracy and precision in photonic Doppler velocimetry. Rev. Sci. Instrum. **81**(053905), 1–7 (2010). doi:10.1063/1.3429257
43. Braithwaite, C.H., Pachman, J., Majzlik, J., Williamson, D.M.: Recalibration of the large scale gap-test to a stress scale. Propellants Explos. Pyrotech. **37**(5), 614–620 (2012). doi:10.1002/prep.201200006
44. Coleburn, N.L.: Chapman–Jouguet pressures of several pure and mixed explosives. NOLTR 64-58, United States Naval Ordnance Laboratory, Maryland, USA, DTIC Accession Number AD0603540 (1964)
45. Majzlík, J., Dusík, V.: DETPAR—The Catalogue of Detonation Parameters, 1st edn. University of Pardubice, Pardubice (2002)